

Simplified Approximation Procedure for Performance-Based Evaluation of Liquefaction Potential

Roy T. Mayfield, M.ASCE¹; Steven L. Kramer, M.ASCE²; and Yi-Min Huang³

Abstract: Performance-based procedures for evaluation of liquefaction potential have been shown to provide more consistent and accurate indications of the actual likelihood of liquefaction in areas of different seismicity than conventional procedures. The process of performing a complete site-specific performance-based evaluation of liquefaction potential, however, requires numerous calculations involving quantities that many geotechnical engineers are not familiar with. This paper shows how the results of complete performance-based analyses can be expressed in terms of a scalar parameter corresponding to a particular element of soil in a reference soil profile, and presents procedures for adjustment of that parameter to account for site-specific conditions that differ from those of the reference profile. The procedures are shown to closely approximate the results of complete site-specific performance-based evaluations. Engineers can then use mapped values of the scalar parameter, along with the recommended adjustment procedure, to realize the benefits of a performance-based evaluation without having to actually perform the performance-based calculations.

DOI: 10.1061/(ASCE)GT.1943-5606.0000191

CE Database subject headings: Earthquakes; Soil liquefaction; Sand, soil type; Penetration tests; Hazards.

Author keywords: Earthquakes; Liquefaction; Sands; Standard penetration tests; Hazard analysis.

Introduction

Evaluation of liquefaction potential has been a topic of considerable interest to geotechnical engineers since its devastating effects were widely observed following 1964 earthquakes in Niigata, Japan, and Alaska. Since that time, a great deal of research on soil liquefaction has been completed in many countries that are exposed to this important seismic hazard. This work has resulted in the development of useful empirical procedures that allow deterministic and probabilistic evaluation of liquefaction potential for a specified level of ground shaking.

The development of performance-based earthquake engineering (PBEE) has provided a framework for more accurate and consistent evaluation of the likelihood of liquefaction at a particular site. Performance-based evaluations of liquefaction potential are developed by integrating probabilistic seismic hazard analyses and probabilistic liquefaction potential analyses. Such evaluations consider all levels of ground shaking ranging from low levels that occur relatively frequently to very high levels that occur only rarely, and the full distribution of magnitude contributing to each level of ground shaking. The result can be expressed in terms of hazard curves for factor of safety against liquefaction or penetra-

tion resistance required to prevent liquefaction (Kramer and Mayfield 2007).

This paper shows how the results of a performance-based liquefaction evaluation procedure can be expressed in terms of a scalar quantity. The scalar parameter corresponding to a reference soil profile can be computed in a complete performance-based analysis and mapped, just as ground motion parameters are currently mapped for building codes and other applications; examples of such maps for Washington State are presented. A procedure to adjust the mapped parameter to represent local site-specific profiles is developed. This procedure allows a user to approximate the results, and thereby realize the benefits, of a performance-based liquefaction potential evaluation without having to perform the voluminous PBEE calculations. The paper ends with a comparison of the results of the site-specific adjustment procedure with those of the full PBEE method.

Conventional Liquefaction Potential Evaluation

In practice, liquefaction potential is usually evaluated deterministically by comparing the cyclic stress ratio (CSR), with a cyclic resistance ratio (CRR). The CSR, which describes the loading applied to the soil, is usually obtained using the "simplified method" in which it can be expressed as

$$\text{CSR} = 0.65 \frac{a_{\max}}{g} \times \frac{\sigma_{vo}}{\sigma'_{vo}} \times \frac{r_d}{\text{MSF}} \quad (1)$$

where a_{\max} =peak ground surface acceleration; g =acceleration of gravity (in same units as a_{\max}); σ_{vo} =initial vertical total stress; σ'_{vo} =initial vertical effective stress; r_d =depth reduction factor; and MSF=magnitude scaling factor, which is a function of earthquake magnitude. The depth reduction factor accounts for compliance of a typical soil profile and the magnitude scaling factor acts as a proxy for the number of significant cycles, which is

¹Consulting Engineer, Kirkland, WA 98034; formerly, Graduate Research Assistant, Univ. of Washington. E-mail: roy@mayfield.name

²Professor, Dept. of Civil and Environmental Engineering, Univ. of Washington, Seattle, WA 98195-2700. E-mail: kramer@u.washington.edu

³Staff Engineer, Landau Associates, Edmonds, WA 98020; formerly, Graduate Research Assistant, Univ. of Washington. E-mail: ninerh@u.washington.edu

Note. This manuscript was submitted on October 6, 2008; approved on July 1, 2009; published online on July 3, 2009. Discussion period open until June 1, 2010; separate discussions must be submitted for individual papers. This paper is part of the *Journal of Geotechnical and Geoenvironmental Engineering*, Vol. 136, No. 1, January 1, 2010. ©ASCE, ISSN 1090-0241/2010/1-140-150/\$25.00.

Table 1. Cetin et al. (2004) Model Coefficients with and without Measurement/Estimation Errors [after Cetin et al. (2002)]

Case	Measurement/estimation errors	θ_1	θ_2	θ_3	θ_4	θ_5	θ_6	σ_ε
I	Included	0.004	13.79	29.06	3.82	0.06	15.25	4.21
II	Removed	0.004	13.32	29.53	3.70	0.05	16.85	2.70

related to the ground motion duration. It should be noted that two pieces of loading information— a_{\max} and earthquake magnitude—are required to compute the CSR.

The CRR value is usually obtained by correlation to penetration resistance or, in some cases, shear wave velocity. Numerous standard penetration test (SPT)-based CRR models, both deter-

ministic (Seed and Idriss 1971; Seed et al. 1985; Youd et al. 2001; Idriss and Boulanger 2004) and probabilistic (Liao et al. 1988; Toprak et al. 1999; Youd and Noble 1997; Juang and Jiang 2000; Cetin et al. 2004) have been developed over the past 40 years. The model of Cetin et al. (2004) treats liquefaction resistance probabilistically, and can be expressed as

$$P_L = \Phi \left[- \frac{(N_1)_{60}(1 + \theta_1 FC) - \theta_2 \ln \text{CSR}_{\text{eq}} - \theta_3 \ln M_w - \theta_4 \ln(\sigma'_{vo}/p_a) + \theta_5 FC + \theta_6}{\sigma_\varepsilon} \right] \quad (2)$$

where P_L =probability of liquefaction; Φ =standard cumulative normal distribution function; $(N_1)_{60}$ =SPT resistance corrected for energy and overburden stress; FC=fines content (in percent); CSR_{eq} is CSR [Eq. (1)] without MSF; M_w =moment magnitude; p_a =atmospheric pressure (in same units as σ'_{vo}); σ_ε =measure of the estimated model and parameter uncertainty for Eq. (2); and θ_1 – θ_6 =model coefficients obtained by regression. Cetin et al. (2002) describe two sets of coefficients for their liquefaction probability model: one with errors from the model and parameter measurement/estimation combined, and one with parameter measurement/estimation errors excluded. Table 1 summarizes both sets of coefficients. CRR curves associated with different P_L levels (with measurement/estimation errors included) are shown in Fig. 1. Cetin et al. (2004) recommend the use of CRR values corresponding to $P_L=15\%$ in their specific deterministic liquefaction potential evaluation procedure.

After determining the appropriate values of CRR and CSR, liquefaction potential is then commonly expressed in terms of a factor of safety against liquefaction defined as

$$\text{FS}_L = \frac{\text{CRR}}{\text{CSR}} \quad (3)$$

In conventional liquefaction potential evaluations, the value of a_{\max} is usually that associated with a single return period (e.g., 475 years) and the value of MSF is usually computed using the mean or modal magnitude from the deaggregation of the a_{\max} hazard at that same return period. A soil deposit is generally considered to have adequate liquefaction resistance if the deterministic factor of safety computed with these parameters exceeds some minimum value, e.g., 1.1–1.3 (e.g., Martin and Lew 1999).

Performance-Based Liquefaction Potential Evaluation

The roots of performance-based liquefaction assessment are in the method of seismic risk analysis introduced by Cornell (1968). The first known application of this approach to liquefaction assessment was presented by Yegian and Whitman (1978), although earthquake loading was described as a combination of earthquake magnitude and source-to-site distance rather than peak acceleration and magnitude. Atkinson et al. (1984) developed a procedure for estimation of the annual probability of liquefaction using linearized approximations of the CRR curves of Seed and Idriss (1983) in a deterministic manner. Marrone et al. (2003) described liquefaction assessment methods that incorporate probabilistic CRR curves and a full range of magnitudes and peak acceleration values. Kramer and Mayfield (2005, 2007) developed a performance-based procedure for liquefaction hazard evaluation using a PBEE framework developed by the Pacific Earthquake Engineering Research Center, and showed that consistent application of the conventional approach led to inconsistent actual liquefaction potential results in different seismic environments. Hwang et al. (2005) described a Monte Carlo simulation-based approach that produced similar results. Baker and Faber (2008) described a performance-based evaluation of liquefaction potential with consideration of spatial variability.

The Kramer and Mayfield (2007) procedure allowed liquefaction hazard to be expressed in two ways—in terms of a factor of

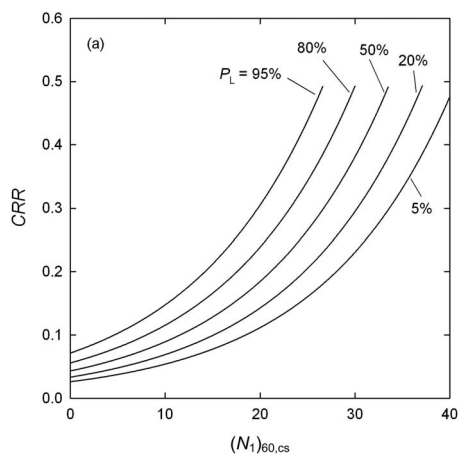


Fig. 1. Relationship between $(N_1)_{60,cs}$, CRR, and probability of liquefaction using Cetin et al. (2004) model ($M_w=7.5$, $\sigma'_{vo}=1$ atm, FC=0, Case I coefficients, Table 1)

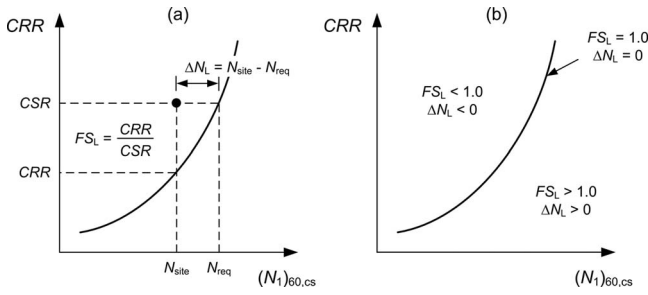


Fig. 2. Schematic illustration of: (a) definitions of FS_L and ΔN_L ; (b) relationship between FS_L and ΔN_L

safety against liquefaction [Eq. (3)] or in terms of a relative penetration resistance

$$\Delta N_L = N_{site} - N_{req} \quad (4)$$

where N_{site} = corrected in situ SPT resistance, $(N_1)_{60,cs}$, for the soil element of interest and N_{req} = corrected SPT resistance to produce

$$P[FS_L < fs_L | a_{max,i}, m_j] = \Phi \left[- \frac{(N_1)_{60}(1 + \theta_1 FC) - \theta_2 \ln(CSR_{eq,i,j} fs_L) - \theta_3 \ln m_j - \theta_4 \ln(\sigma'_{vo}/p_a) + \theta_5 FC + \theta_6}{\sigma_e} \right] \quad (6)$$

Given that liquefaction is expected to occur when $\Delta N_L < 0$ (i.e., when $N_{site} < N_{req}$), or when $FS_L < 1.0$, then $P_L = P[\Delta N_L < 0] = P[FS_L < 1.0]$. The PBEE approach can then be applied in such a way as to produce a mean annual rate of exceedance of $N_{req} = n_{req}$. Using the Cetin et al. (2004) model

$$\lambda_{N_{req}}(n_{req}) = \sum_{j=1}^{N_M} \sum_{i=1}^{N_{a_{max}}} P[N_{req} > n_{req} | a_{max,i}, m_j] \Delta \lambda_{a_{max,i}, m_j} \quad (7)$$

where

$$P[N_{req} > n_{req} | a_{max,i}, m_j] = \Phi \left[- \frac{n_{req} - \theta_2 \ln CSR_{eq,i,j} - \theta_3 \ln m_j - \theta_4 \ln(\sigma'_{vo}/p_a) + \theta_6}{\sigma_e} \right] \quad (8)$$

with $n_{req} = (N_1)_{60,cs} = (N_1)_{60}(1 + \theta_2 FC) + \theta_5 FC$. The value of n_{req} can be interpreted as the corrected clean sand SPT resistance required to prevent initiation of earthquake-induced liquefaction with a return period of $1/\lambda_{N_{req}}(n_{req})$.

Liquefaction Hazard Curves

Kramer and Mayfield (2007) described the development of liquefaction hazard curves, i.e., plots showing the mean annual rate of nonexceedance of different factors of safety and the mean annual rate of exceedance of different values of N_{req} . Fig. 3 shows a simple, idealized, reference soil profile, and FS_L and N_{req} hazard curves for an element of soil at a depth of 6 m in that profile if it was located in Seattle. The assumed SPT resistance of that element is $N_{site} = 18$ and the seismic hazard information is from the USGS 2002 interactive deaggregation Web site ([\$FS_L = 1.0\$ for the same soil element. Fig. 2 illustrates the relationship between \$FS_L\$ and \$\Delta N_L\$; it is apparent that either \$FS_L\$ or \$\Delta N_L\$ can be used as indicators of liquefaction potential.](http://</p>
</div>
<div data-bbox=)

Kramer and Mayfield (2007) showed that the mean annual rate of nonexceedance of a selected factor of safety, $FS_L = fs_L$, could be computed as

$$\Lambda_{FS_L}(fs_L) = \sum_{j=1}^{N_M} \sum_{i=1}^{N_{a_{max}}} P[FS_L < fs_L | a_{max,i}, m_j] \Delta \lambda_{a_{max,i}, m_j} \quad (5)$$

where N_M and $N_{a_{max}}$ = number of magnitude and peak acceleration increments into which the “hazard space” is subdivided and $\Delta \lambda_{a_{max,i}, m_j}$ is the incremental mean annual rate of exceedance for intensity measure, $a_{max,i}$, and magnitude, m_j . The value of $\Lambda_{FS_L}(fs_L)$ increases with increasing fs_L since weaker motions producing higher factors of safety occur more frequently than stronger motions that produce lower factors of safety. The conditional probability term in Eq. (5) was calculated using the probabilistic model of Cetin et al. (2004) with $CSR_{eq,i,j}$ computed from $a_{max,i}$ and $M_w = m_j$, i.e.

eqint.cr.usgs.gov/deaggint/2002/index.php), which provides peak acceleration data for soft rock ($V_{s,30} = 760$ m/s) conditions and the deaggregated contributions from a range of magnitudes. The hazard curve for FS_L [Fig. 3(b)] shows that the factor of safety against liquefaction would be expected to drop below 1.0 at a mean annual rate of $0.00695 \text{ year}^{-1}$; hence, the return period of liquefaction for that element of soil would be 144 years. Fig. 3(b) also shows that the 475-year factor of safety (i.e., the factor of safety for $\lambda_{FS_L} = 1/475$) is 0.55. Fig. 3(c) shows that this element of soil with a corrected penetration resistance of 26.2 blows/ft would be expected to undergo liquefaction every 475 years (on average) in Seattle. These hazard curves can be used in the same manner as conventional ground motion hazard curves, e.g., to compute probabilities of exceedance (or nonexceedance) in various periods of time.

Liquefaction Parameter Maps

Liquefaction hazard curves, such as those shown in Fig. 3, can be used to compute values of FS_L or N_{req} associated with a particular return period at a particular location. Calculating the value of FS_L requires knowledge of N_{site} , but calculating the value of N_{req} does not. By assuming a reference soil profile at different locations and computing N_{req} hazard curves for each of those locations, a liquefaction parameter map can be constructed. Fig. 4 shows contours of N_{req}^{ref} values for the 6-m-deep element in the reference profile of Fig. 3(a) corresponding to return periods of 475 and 2,475 years in Washington State. Hereafter, the superscripts in N_{req}^{ref} and N_{req}^{site} will be used to distinguish between N_{req} values for the reference profile and a site-specific profile. The contours were developed from N_{req}^{ref} values computed at 247 locations on a grid spaced at 0.3° latitude and 0.5° longitude across the state using

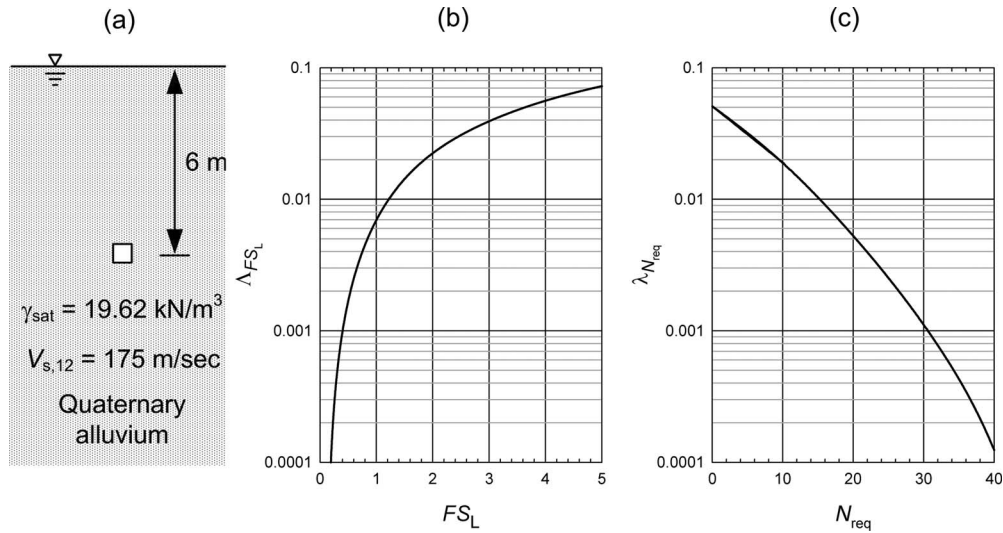


Fig. 3. (a) Idealized reference profile with $N_{\text{site}}=18$; (b) hazard curve for FS_L ; and (c) hazard curve for N_{req} in Seattle

PSHA results obtained from the USGS 2002 interactive deaggregation website. The soft rock peak accelerations were adjusted by applying the Stewart et al. (2003) median amplification factor

$$F_a = \exp(a + b \ln a_{\text{max,rock}}) \quad (9)$$

with the coefficients for Quaternary alluvium ($a=-0.15$, $b=-0.13$). The shapes of the $N_{\text{req}}^{\text{ref}}$ contours generally reflect the known seismicity of Washington State, which is dominated by the Cascadia Subduction Zone in which the Juan de Fuca plate subducts beneath the curved boundary of the North American plate

along coastal Washington (as well as British Columbia to the north and Oregon to the south).

Site-Specific N_{req} Adjustments

The mapped $N_{\text{req}}^{\text{ref}}$ values shown in Fig. 4 correspond to the particular element of soil at 6-m depth in the reference soil profile shown in Fig. 3(a). In order to be broadly useful, the mapped $N_{\text{req}}^{\text{ref}}$ values must be adjusted to provide site-specific N_{req} values for elements at depths other than 6 m in profiles with characteristics different than those of the reference profile. Recalling Eq. (2) with coefficients from Table 1 with measurement/estimation errors included, and letting $(N_1)_{60,cs}^{\text{Cetin}} = (N_1)_{60}(1+0.004FC) + 0.06FC$, then

$$(N_1)_{60,cs}^{\text{Cetin}} = 13.79 \ln \text{CSR}_{\text{eq}} + 29.06 \ln M_w + 3.82 \ln \frac{\sigma'_{vo}}{p_a} - 15.25 - 4.21\Phi^{-1}(P_L) \quad (10)$$

Letting $N_{\text{req}} = (N_1)_{60,cs}^{\text{Cetin}}$ and using the definition of CSR_{eq} , the value of $N_{\text{req}}^{\text{ref}}$ can be described as

$$N_{\text{req}}^{\text{ref}} = 13.79 \ln \left(0.65 F_a^{\text{ref}} a_{\text{max,rock}}^{\text{ref}} \frac{\sigma'_{vo}}{(\sigma'_{vo})_{\text{ref}}} r_d^{\text{ref}} \right) + 29.06 \ln M_w + 3.82 \ln \frac{(\sigma'_{vo})_{\text{ref}}}{p_a} - 15.25 - 4.21\Phi^{-1}(P_L) \quad (11)$$

Similarly, the value of $N_{\text{req}}^{\text{site}}$ can be expressed as

$$N_{\text{req}}^{\text{site}} = 13.79 \ln \left(0.65 F_a^{\text{site}} a_{\text{max,rock}}^{\text{site}} \frac{\sigma'_{vo}}{(\sigma'_{vo})_{\text{ref}}} r_d^{\text{site}} \right) + 29.06 \ln M_w + 3.82 \ln \frac{(\sigma'_{vo})_{\text{site}}}{p_a} - 15.25 - 4.21\Phi^{-1}(P_L) \quad (12)$$

Note that the stress, amplification factor and r_d terms in these equations are different, but the other terms are the same.

The site-specific adjustment can be expressed in terms of a blowcount adjustment, ΔN_{req} , defined such that

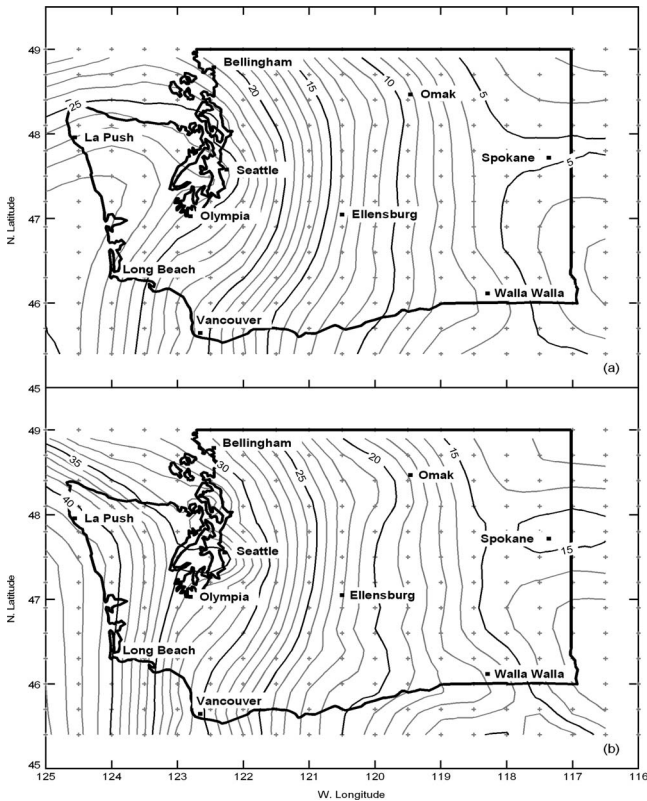


Fig. 4. Contours of $N_{\text{req}}^{\text{ref}}$ for Washington State: (a) 475-year return period; (b) 2,475-year return period

$$N_{\text{req}}^{\text{site}} = N_{\text{req}}^{\text{ref}} + \Delta N_{\text{req}} \quad (13)$$

Therefore, subtracting $N_{\text{req}}^{\text{ref}}$ from both sides and substituting Eqs. (11) and (12), the blowcount adjustment can be written as

$$\begin{aligned} \Delta N_{\text{req}} = & 13.79 \ln \left(\frac{\sigma_{vo}^{\text{site}} / (\sigma_{vo}')^{\text{site}}}{\sigma_{vo}^{\text{ref}} / (\sigma_{vo}')^{\text{ref}}} \right) + 3.82 \ln \left(\frac{(\sigma_{vo}')^{\text{site}}}{(\sigma_{vo}')^{\text{ref}}} \right) + 13.79 \ln \frac{F_a^{\text{site}}}{F_a^{\text{ref}}} \\ & + 13.79 \ln \frac{r_d^{\text{site}}}{r_d^{\text{ref}}} \end{aligned} \quad (14)$$

The terms in the blowcount adjustment can be grouped into components associated with vertical stresses, amplification behavior, and depth reduction factor behavior, giving

$$\Delta N_{\text{req}} = \Delta N_{\sigma} + \Delta N_F + \Delta N_{r_d} \quad (15)$$

where

$$\Delta N_{\sigma} = 13.79 \ln \left(\frac{\sigma_{vo}^{\text{site}} / (\sigma_{vo}')^{\text{site}}}{\sigma_{vo}^{\text{ref}} / (\sigma_{vo}')^{\text{ref}}} \right) + 3.82 \ln \left(\frac{(\sigma_{vo}')^{\text{site}}}{(\sigma_{vo}')^{\text{ref}}} \right)$$

$$\Delta N_F = 13.79 \ln \frac{F_a^{\text{site}}}{F_a^{\text{ref}}}$$

$$\Delta N_{r_d} = 13.79 \ln \frac{r_d^{\text{site}}}{r_d^{\text{ref}}}$$

This formulation allows a user to obtain $N_{\text{req}}^{\text{ref}}$ at a site of interest from a map such as that shown in Fig. 4, and then to determine $N_{\text{req}}^{\text{site}}$ using a blowcount adjustment procedure. Two adjustment procedures, which require different levels of effort to implement, are described in the following sections.

Adjustment Procedure A

Substituting the reference site conditions into the individual components of the blowcount adjustment, the stress and amplification components can be expressed as

$$\Delta N_{\sigma} = 13.79 \ln \left(\frac{\sigma_{vo}^{\text{site}} / (\sigma_{vo}')^{\text{site}}}{2} \right) + 3.82 \ln \left(\frac{(\sigma_{vo}')^{\text{site}}}{p_a} \right) + 2.07 \quad (16)$$

$$\Delta N_F = 13.79 \ln \frac{F_a^{\text{site}}}{F_a^{\text{ref}}} = 13.79 [a^{\text{site}} + 0.15 + (b^{\text{site}} + 0.13) \ln a_{\text{max,rock}}] \quad (17)$$

Cetin et al. (2004) considered the variation of cyclic shear stress with depth to be influenced by peak acceleration, earthquake magnitude, and average shear wave velocity within the upper 12 m of a soil profile. They expressed the mean value of their depth reduction factor model as

$$r_d^{\text{site}} = \frac{1 + \frac{-23.013 - 2.949a_{\text{max}} + 0.999M_w + 0.0525\bar{V}_{s,12}}{16.258 + 0.201 \exp[0.341(-z + 0.0785\bar{V}_{s,12} + 7.586)]}}{1 + \frac{-23.013 - 2.949a_{\text{max}} + 0.999M_w + 0.0525\bar{V}_{s,12}}{16.258 + 0.201 \exp[0.341(0.0785\bar{V}_{s,12} + 7.586)]}} \quad (18)$$

where $\bar{V}_{s,12}$ = average shear wave velocity over the upper 12 m of the profile. This expression includes the variables a_{max} and M_w ,

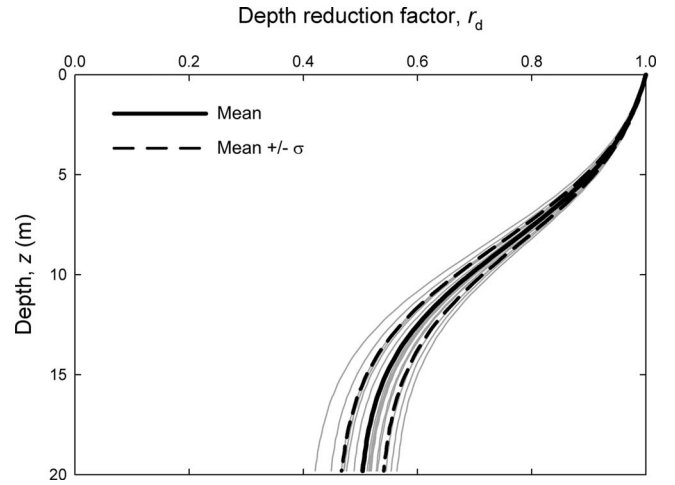


Fig. 5. Computed mean r_d profiles with $V_{s,12} = 175$ m/s for 475-year and 2,475-year peak acceleration and mean magnitude for Butte, Mont.; Charleston, S.C.; Eureka, Calif.; Memphis, Tenn.; Portland, Ore.; Salt Lake City; San Francisco; San Jose, Calif.; Santa Monica, Calif.; and Seattle

which are used in the $N_{\text{req}}^{\text{ref}}$ integration [Eq. (7)]. Parametric studies indicate that r_d is relatively insensitive to combinations of a_{max} and M_w that typically affect liquefaction hazards; an observation at least partly explained by the fact that both variables affect the numerator and denominator of the r_d expression similarly. Fig. 5 shows mean r_d values for 20 combinations of a_{max} and M_w that represent the 475- and 2,475-year peak accelerations and mean (deaggregated) magnitudes for 10 cities across the United States. Even with a_{max} values ranging from 0.12g to 1.02g and mean M_w values ranging from 5.97 to 7.70, the mean r_d values fall within a relatively narrow range. Substituting $a_{\text{max}} = 0.39g$ and $M_w = 6.5$ into Eq. (18) produces r_d^{site} values that match the mean curve shown in Fig. 5 very closely (maximum error of 0.08%). Due to this lack of sensitivity, it is reasonable to compute r_d^{site} for Adjustment Procedure A using the ground surface a_{max} value and mean M_w value corresponding to the return period of interest instead of computing it for each combination of a_{max} and M_w in the N_{req} integration

$$\Delta N_{r_d} = 13.79 \ln \frac{r_d^{\text{site}}}{0.866} \quad (19)$$

With Eqs. (16), (17), and (19), computing the blowcount adjustment involves computing the site-specific total and effective vertical stresses at the depth of interest, determining the appropriate site amplification coefficients within the framework of the Stewart et al. (2003) expression [Eq. (9)], and computing the Cetin et al. value of r_d at the depth of interest.

Adjustment Procedure B

Since both stresses and r_d vary significantly with depth, the development of a simpler alternative adjustment procedure was investigated. The intent of this alternative was to produce simplified depth-related expressions for ΔN_{σ} and ΔN_{r_d} that could be expressed in chart form for rapid estimation of those quantities. The ΔN_F adjustment for Procedure B is the same as for Procedure A and is not repeated in the following discussion.

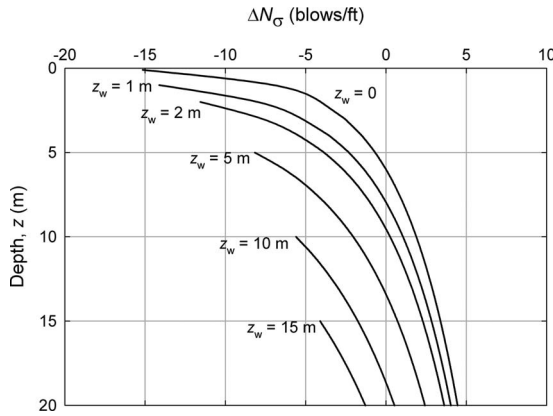


Fig. 6. Stress-related component of Adjustment Procedure B

Stress Component

The densities of most inorganic soils fall within a relatively narrow range, at least compared to many other soil properties. For a site with a uniform density profile and a groundwater table at depth, $z=z_w$, the initial total and effective vertical stresses are given by

$$\sigma_{vo}^{\text{site}} = \gamma_d z_w + \gamma_{\text{sat}}(z - z_w) \quad (20a)$$

$$(\sigma'_{vo})^{\text{site}} = \gamma_d z_w + \gamma_b(z - z_w) \quad (20b)$$

where the dry unit weight, γ_d , saturated unit weight, γ_{sat} , and buoyant unit weight, γ_b , are functions of soil void ratio (and specific gravity of solids and unit weight of water, which are assumed to be constants). The ratio of total to effective vertical stress at some depth, $z \geq z_w$, can therefore be written as

$$\Delta N_{r_d} = 13.79 \left\{ \ln \left[\frac{-1.353 + 0.0525 \bar{V}_{s,12} + 2.671 \exp(0.0268 \bar{V}_{s,12} - 0.341z)}{-1.353 + 0.0525 \bar{V}_{s,12} + 2.671 \exp(0.0268 \bar{V}_{s,12})} \right] \right\} \quad (26)$$

Fig. 7 shows the variation of ΔN_{r_d} with depth and shear wave velocity; this component of the correction can be seen to be quite sensitive to both depth and mean shear wave velocity.

Discussion

The site specific components of the blowcount adjustment—vertical stress, amplification factor, and r_d —are all contained in the Cetin et al. (2004) relationship for probability of liquefaction. Through consistent use of this relationship in the full perfor-

$$\frac{\sigma_{vo}^{\text{site}}}{(\sigma'_{vo})^{\text{site}}} = \frac{G_s + e^{\text{site}}(1 - z_w/z)}{G_s - 1 + z_w/z} \quad (21)$$

For the reference site, $G_s^{\text{ref}}=2.67$, $e^{\text{ref}}=0.67$, $z_w=0$, and $\sigma_{vo}^{\text{ref}}/(\sigma'_{vo})^{\text{ref}}=2$, so

$$\frac{\sigma_{vo}^{\text{site}}/(\sigma'_{vo})^{\text{site}}}{\sigma_{vo}^{\text{ref}}/(\sigma'_{vo})^{\text{ref}}} = \frac{G_s + e^{\text{site}}(1 - z_w/z)}{2(G_s - 1 + z_w/z)} \quad (22)$$

and

$$\frac{(\sigma'_{vo})^{\text{site}}}{(\sigma'_{vo})^{\text{ref}}} = \frac{z(G_s - 1 + z_w/z)}{6(1 + e^{\text{site}})} \quad (23)$$

Therefore

$$\Delta N_{\sigma} = 13.79 \ln \left[\frac{G_s + e^{\text{site}}(1 - z_w/z)}{2(G_s - 1 + z_w/z)} \right] + 3.82 \ln \left[\frac{z(G_s - 1 + z_w/z)}{6(1 + e^{\text{site}})} \right] \quad (24)$$

Assuming that G_s and e^{site} are the same as in the reference profile, the expression for ΔN_{σ} depends solely on z and z_w , i.e.

$$\Delta N_{\sigma} = 13.79 \ln \left[\frac{1 - 0.2z_w/z}{1 + 0.6z_w/z} \right] + 3.82 \ln \left[\frac{z}{6} (1 + 0.6z_w/z) \right] \quad (25)$$

Fig. 6 illustrates the variation of ΔN_{σ} with depth for different groundwater table depths using Eq. (25). The sensitivity of Eq. (24) to e^{site} is quite low—an e^{site} value of 0.8 (very loose for most naturally deposited sands) would increase ΔN_{σ} by only 0.23 blows/ft, and an e^{site} value of 0.5 (quite dense for most potentially liquefiable sands) would decrease ΔN_{σ} by 0.29 blows/ft; this insensitivity suggests that the assumption of $e^{\text{site}}=e^{\text{ref}}$ should not significantly affect the accuracy of ΔN_{σ} .

Depth Reduction Factor Component

Fig. 5 showed the relative insensitivity of r_d to a_{max} and M_w . Using a combination of a_{max} and M_w that correspond to the mean curve in Fig. 5, and recognizing that the reference profile has $\bar{V}_{s,12}^{\text{ref}}=175$ m/s, $z^{\text{ref}}=6$ m, and $r_d^{\text{ref}}=0.866$, the depth reduction factor adjustment component can be written as a function of only depth and mean shear wave velocity

mance-based calculation of $N_{\text{req}}^{\text{ref}}$ and in the development of the blowcount adjustment, the details of the reference site profile are of minor importance. Changing the reference site profile will change $N_{\text{req}}^{\text{ref}}$, but it will also change the blowcount adjustments by an equivalent amount so that, for all practical purposes, the same $N_{\text{req}}^{\text{site}}$ is obtained. The verification process described later in this paper will show that even the simplifying assumptions about r_d and soil void ratio are of minor consequence when the relationship for probability of liquefaction is consistently applied.

Relationship between ΔN_L and FS_L

Using mapped values of N_{req}^{ref} and either of the previously discussed adjustment procedures, site-specific estimates of $\Delta N_L = N_{site} - N_{req}^{site}$ can be obtained for a particular element of soil. While ΔN_L was shown previously to provide the same basic information as FS_L , most engineers are accustomed to expressing liquefaction potential in terms of a factor of safety. Therefore, it is

useful to relate ΔN_L to FS_L . The site-specific factor of safety can be written as

$$FS_L^{site} = \frac{CRR}{CSR} = \frac{CRR(N_{site})}{CRR(N_{req}^{site})} \quad (27)$$

The Cetin et al. (2004) model can be rearranged to express CRR as

$$CRR = \exp \left[\frac{N_{req}^{Cetin} - 29.06 \ln M_w - 3.82 \ln \left(\frac{\sigma'_{vo}}{p_a} \right) + 15.25 + \sigma_\epsilon \Phi^{-1}(P_L)}{13.79} \right] \quad (28)$$

Substituting Eq. (28) and the appropriate values of penetration resistance into Eq. (27) gives

$$FS_L^{site} = \frac{\exp \left[\frac{N_{site} - 29.06 \ln M_w - 3.82 \ln \left(\frac{\sigma'_{vo}}{p_a} \right) + 15.25 + \sigma_\epsilon \Phi^{-1}(P_L)}{13.79} \right]}{\exp \left[\frac{N_{req}^{site} - 29.06 \ln M_w - 3.82 \ln \left(\frac{\sigma'_{vo}}{p_a} \right) + 15.25 + \sigma_\epsilon \Phi^{-1}(P_L)}{13.79} \right]} = \exp \left[\frac{N_{site} - N_{req}^{site}}{13.79} \right] = 1.075^{\Delta N_L} \quad (29)$$

The exponential nature of the Cetin et al. (2004) CRR relationship, therefore, provides a conveniently simple relationship between FS_L^{site} and ΔN_L .

Verification of Site-Specific Adjustment Procedures

The site-specific adjustments yield N_{req} values that can differ from those that would be obtained from a complete, site-specific, performance-based liquefaction potential evaluation. In the complete analysis, uncertainties in source parameters (e.g., earthquake magnitude) and ground motion parameter (e.g., peak acceleration) are combined with a probabilistic liquefaction potential analysis to yield N_{req} values with a rigorously characterized mean annual rate of exceedance (or return period). The proposed adjustment

procedures, however, are applied deterministically, i.e., they are based on mean (or median) relationships without explicit consideration of the dispersion about the mean (or median). The proposed Adjustment Procedure B also makes assumptions about the variations of stresses and r_d with depth that may be different than those in a complete, site-specific performance-based evaluation.

The following sections compare the results of liquefaction potential evaluations performed using the full site-specific, performance-based procedure with those obtained from mapped reference profile N_{req} values processed by both of the proposed adjustment procedures.

Soil Profile

Fig. 8 shows a profile from an actual site along the Seattle waterfront. The profile consists of 1.5 m of medium dense, sandy silt underlain by about 9 m of generally loose, silty, fine to coarse sand (5–10% nonplastic fines) placed by hydraulic filling. This material is underlain by about 3.6 m of natural sandy silt (80% nonplastic fines), which lies on top of a thick sequence of very dense, glacially overconsolidated, silty, and gravelly sands. The groundwater level is at about 2.4 m and the silts at the site are generally nonplastic. The computed value of $V_{s,12}$ from the shear wave velocity profile in Fig. 8 is 137 m/s.

Site-Specific Liquefaction Potential

Fig. 9 shows FS_L^{site} and N_{req}^{site} hazard curves for elements of soil at depths of 4.3 m ($N_{site} = 10.9$ blows/ft) and 8.2 m ($N_{site} = 2.7$ blows/ft). These hazard curves were computed using the procedure of Kramer and Mayfield (2007) and are therefore fully site specific, i.e., they were computed for each depth considering the specific properties of the site. The hazard curves indicate 475-year factors of safety of 0.53 and 0.28 for the shallower and

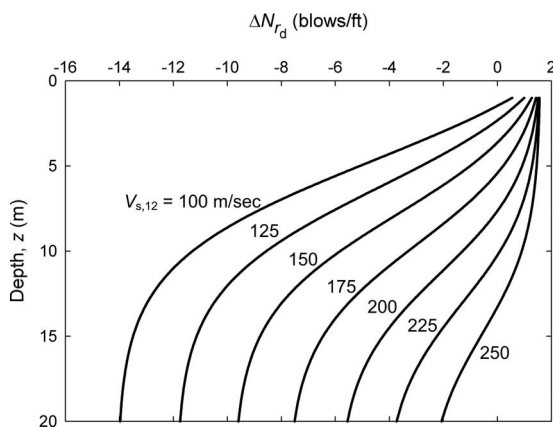


Fig. 7. Depth reduction factor-related component of Adjustment Procedure B

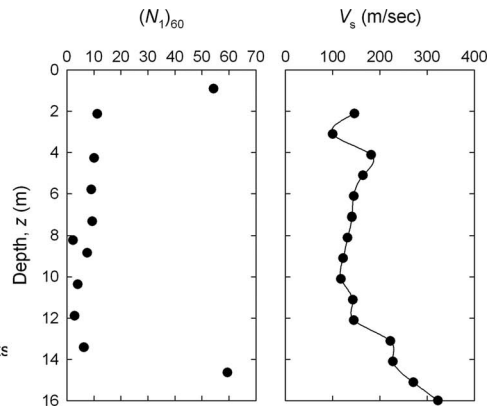
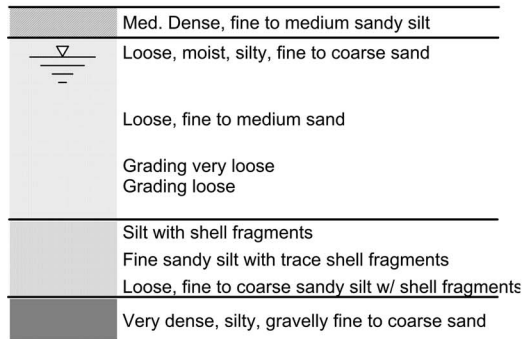


Fig. 8. Soil profile from Seattle waterfront

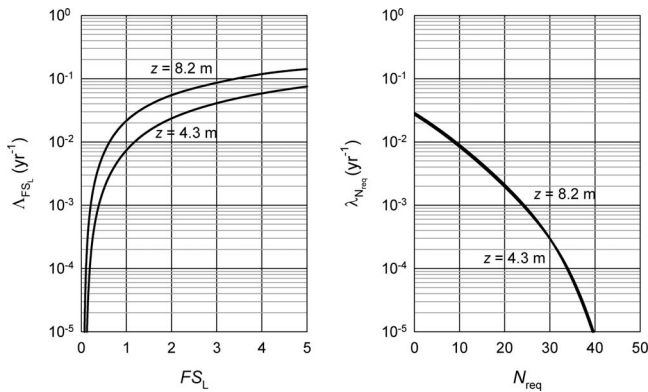


Fig. 9. Hazard curves for FS_L and N_{req} for two elements of soil in Seattle waterfront profile

Table 2. Directly Computed Site-Specific Liquefaction Hazard Parameters

Depth (m)	N_{site}	475-year N_{req}^{site}	475-year FS_L^{site}	$T_{R,liq}$
4.3	10.9	19.5	0.54	135
5.8	9.7	20.3	0.46	104
7.3	10.1	20.2	0.48	110
8.2	2.7	20.0	0.28	46
8.8	8.2	19.9	0.43	90
10.4	7.1	19.5	0.41	82
11.9	5.5	19.3	0.37	69
13.4	10.1	19.3	0.51	124

deeper elements, respectively; the return periods of liquefaction for the respective elements are 135 and 46 years. The 475-year N_{req}^{site} values are 19.5 and 20.0 blows/ft. Table 2 presents similar data for elements at the depths of each of the SPT tests in the saturated soils above the very dense glacial soils.

The 475-year N_{req}^{site} values can be seen to vary mildly with depth from values of 19.3 at the bottom of the profile to 20.3 at 5.8 m. The 475-year FS_L^{site} values reflect the in situ SPT resistances and, therefore, fluctuate with depth from a high of 0.54 to a low of 0.28 depending on the in situ penetration resistances. Return periods of liquefaction for this profile range from 46 to 135 years. These relatively short return periods are consistent with the observation of localized liquefaction in this general area in the 1949 Olympia, 1965 Seattle-Tacoma, and 2001 Nisqually earthquakes.

The N_{req}^{site} values obtained using both adjustment procedures are shown in Table 3. The N_{req}^{site} values obtained from the two adjustment procedures are in generally good agreement with those obtained from the direct, site-specific analysis [Fig. 10(a)]. The values from Adjustment Procedure A are in excellent agreement at shallow depths, but underpredict the directly obtained values by 0.9 blow/ft at the bottom of the profile. The values from Adjustment Procedure B underpredict the directly obtained values by amounts ranging from about 0.5 blow/ft at shallow depths to 1.3 blows/ft at the bottom of the profile.

Table 4 presents 475-year FS_L values obtained using the adjusted values and the relationship between FS_L and ΔN_L given in Eq. (29). Following from the agreement in N_{req}^{site} values, the 475-year factor of safety values inferred from the ΔN_L values using

Table 3. Site-Specific Required SPT Resistances by Adjustments to 475-Year Seattle N_{req}^{ref} Value of 26.2

Depth (m)	N_{site}	Procedure A				Procedure B			
		ΔN_{σ}	$\Delta N_{r,d}$	ΔN_{req}	$N_{req}^{site,A}$	ΔN_{σ}	$\Delta N_{r,d}$	ΔN_{req}	$N_{req}^{site,B}$
4.3	10.9	-5.8	-0.6	-6.5	19.8	-5.9	-1.2	-7.1	19.1
5.8	9.7	-3.7	-2.2	-5.8	20.4	-3.5	-2.8	-6.4	19.8
7.3	10.1	-2.2	-3.9	-6.0	20.2	-2.0	-4.6	-6.6	19.6
8.2	2.7	-1.4	-4.9	-6.4	19.8	-1.2	-5.7	-6.9	19.3
8.8	8.2	-1.0	-5.6	-6.6	19.6	-0.8	-6.3	-7.1	19.1
10.4	7.1	-0.1	-7.1	-7.2	19.0	0.1	-7.8	-7.7	18.5
11.9	5.5	0.6	-8.3	-7.6	18.6	0.9	-9.0	-8.1	18.1
13.4	10.1	1.3	-9.1	-7.8	18.4	1.6	-9.8	-8.2	18.0

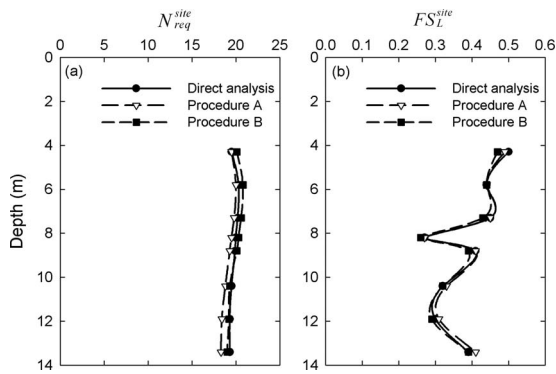


Fig. 10. Comparison of results of direct PBEE analysis and results obtained from mapped N_{req} values: (a) 475-year N_{req}^{site} , (b) 475-year FS_L^{site}

Adjustment Procedure A are in excellent agreement [Fig. 10(b)] with those obtained from the direct, site-specific analysis, particularly at shallower depths.

The soil profile shown in Fig. 8 was then assumed to be located in the same 10 cities used to illustrate performance-based initiation procedures by Kramer and Mayfield (2007). Table 5 shows the mapped N_{req}^{ref} values for each of these sites and the a_{max} and mean M_w values required for Adjustment Procedure A. These cities span a wide range of seismic activity and contain different tectonic settings. Applying the adjustment procedures to the mapped N_{req}^{ref} values for both 475- and 2,475-year return periods and comparing with the directly computed N_{req}^{site} values at all eight depths yields the results shown in Fig. 11. The adjusted N_{req}^{site} values are generally very close to the directly computed values—

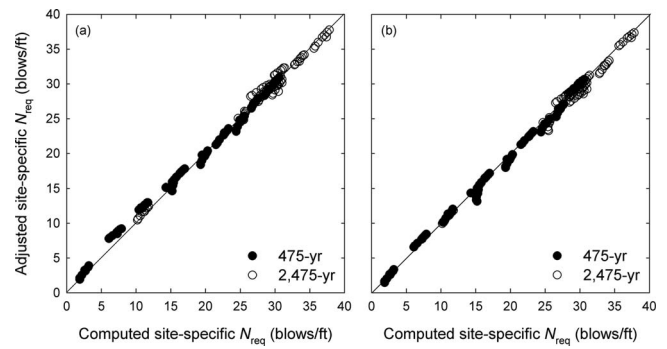


Fig. 11. Relationship between adjusted and directly computed site-specific N_{req} values for 10 U.S. cities: (a) Adjustment Procedure A; (b) Adjustment Procedure B

Adjustment Procedure A has a slight bias toward overprediction with a standard deviation of the differences of 0.68; Adjustment Procedure B has a slight bias toward underprediction with a standard deviation of 0.62 blows/ft. The overprediction by Adjustment Procedure A is dominated by results from two cities (Charleston and Memphis, which produce the groups of points at $N_{req}=6-9$ and 11-14, respectively) at the 475-year hazard level; the highly skewed nature of the deaggregated magnitude distributions for these two cities, whose seismicity is dominated by large, historical earthquakes, gives rise to unusual combinations of a_{max} and mean magnitude (see Table 5) that produce high r_d values that are responsible for the larger difference between the computed and adjusted N_{req} values. Fig. 12 shows comparisons of the directly computed FS_L^{site} values with the values inferred from the adjusted N_{req}^{site} values and Eq. (27). As can be seen, the inferred

Table 4. Site-Specific Factor of Safety Values Inferred from Reference Profile Required SPT Resistance

Depth (m)	N_{site}	475-year FS_L^{site}	Procedure A			Procedure B		
			$N_{req}^{site,A}$	$\Delta N_L^{site,A}$	$FS_L^{site,A}$	$N_{req}^{site,B}$	$\Delta N_L^{site,B}$	$FS_L^{site,B}$
4.3	10.9	0.54	19.8	-8.9	0.53	19.1	-8.3	0.55
5.8	9.7	0.46	20.4	-10.7	0.46	19.8	-10.2	0.48
7.3	10.1	0.48	20.2	-10.1	0.48	19.6	-9.6	0.50
8.2	2.7	0.28	19.8	-17.2	0.29	19.3	-16.6	0.30
8.8	8.2	0.43	19.6	-11.4	0.44	19.1	-10.9	0.45
10.4	7.1	0.41	19.0	-11.9	0.42	18.5	-11.4	0.44
11.9	5.5	0.37	18.6	-13.1	0.39	18.1	-12.6	0.40
13.4	10.1	0.51	18.4	-8.3	0.55	18.0	-7.9	0.57

Table 5. Mapped N_{req}^{ref} and Ground Response Parameters for 10 U.S. Cities

Location	Latitude	Longitude	475-year			2,475-year		
			N_{req}^{ref}	a_{max}	M_w	N_{req}^{ref}	a_{max}	M_w
Butte, Mont.	46.003	112.533	9.7	0.120	5.97	18.2	0.225	6.05
Charleston, S.C.	32.776	79.931	14.8	0.189	6.61	35.6	0.734	7.00
Eureka, Calif.	40.802	124.162	37.0	0.658	7.06	43.7	1.023	7.02
Memphis, Tenn.	35.149	90.048	18.4	0.214	7.01	37.6	0.655	7.26
Portland, Ore.	45.523	122.675	21.4	0.204	6.81	31.5	0.398	6.73
Salt Lake City	40.755	111.898	23.5	0.298	6.69	35.5	0.679	6.76
San Francisco	37.775	122.418	33.5	0.468	7.43	39.7	0.675	7.50
San Jose, Calif.	37.339	121.893	31.3	0.449	6.73	36.5	0.618	6.65
Santa Monica, Calif.	34.015	118.492	29.5	0.432	6.62	36.3	0.710	6.55
Seattle, Wash.	47.530	122.300	26.2	0.332	6.57	35.2	0.620	6.74

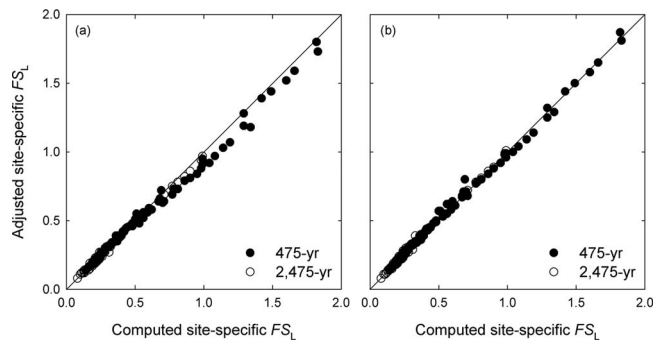


Fig. 12. Relationship between adjusted and directly computed site-specific FS_L values for 10 U.S. cities: (a) Adjustment Procedure A; (b) Adjustment Procedure B

values match the directly computed values very well; the Charleston and Memphis points are responsible for the most underpredicted FS_L^{site} values at the 475-year level. Here, Adjustment Procedures A and B have slight biases toward underprediction and overprediction, respectively—the respective standard deviations of the FS_L^{site} differences for Adjustment Procedures A and B are 0.03 and 0.02.

These results show that the site-specific adjustments, in combination with the mapped N_{req}^{ref} values, produce results that are very close to those obtained by performing complete performance-based liquefaction potential evaluations. Adjustment Procedure A shows slightly better (lower and more conservative bias) agreement with the results of complete performance-based evaluations, but the difference appears to be negligible for practical purposes. They also show that the site-specific N_{req} values can be used with in situ SPT resistances to compute factors of safety. The availability of mapped N_{req}^{ref} values would, therefore, provide a reasonable approximation of performance-based procedures for evaluation of liquefaction potential without requiring the user to perform the numerous calculations involved in those procedures.

Summary and Conclusions

Performance-based procedures for evaluation of liquefaction potential have been shown to provide more accurate and consistent estimates of the likelihood of liquefaction in different seismic environments than conventional procedures. Realization of the benefits of a performance-based evaluation for a particular site, however, requires that the user delve into the results of probabilistic seismic hazard analyses to extract relevant peak acceleration and magnitude data for a range of ground motion return periods. The performance-based calculations, while not inherently difficult (or significantly different than those used in conventional probabilistic liquefaction potential evaluations) are voluminous, time consuming, and unfamiliar to nonspecialists.

This paper has described a methodology by which a scalar quantity, expressed here as the penetration resistance required to prevent initiation of liquefaction in a particular element of soil within a reference soil profile, can be computed and mapped over a desired geographic region. It then describes two alternative procedures by which the mapped parameter can be adjusted for the effects of actual soil conditions to develop site-specific values of the required penetration resistance and inferred factor of safety. Finally, the accuracies of the site-specific adjustment procedures

are demonstrated by applying them to an actual soil profile at different return periods in different seismic environments. A number of conclusions can be drawn from the results of this investigation:

1. The use of a “capacity-related” parameter, such as required SPT resistance, can be useful for liquefaction potential evaluation. The required penetration resistance is independent of the in situ penetration resistance and therefore exhibits smooth and gradual spatial variation that leads to smoother contours when mapped for a given hazard level.
2. A performance-based value of required penetration resistance, i.e., a value that reflects the contributions of all peak accelerations and magnitudes contributing to ground shaking hazards and the uncertainty in liquefaction resistance, can be computed and mapped by a person familiar with the performance-based liquefaction potential evaluation process.
3. The relatively consistent and smoothly varying ratio of total to effective vertical stress and depth reduction factor in typical liquefiable profiles, along with the relative insensitivity of the depth reduction factor to peak acceleration and magnitude, allow required penetration resistances at different depths in a soil profile to be related to each other in a predictable manner.
4. The basic equations on which available probabilistic liquefaction potential evaluation procedures are based can be manipulated to establish well-grounded adjustment factors that relate required penetration resistances and factors of safety for a reference profile to those for a site-specific profile.
5. Testing of the adjustment procedures at different depths, return periods, and seismic environments shows very good agreement with required penetration resistances and factors of safety directly computed from complete performance-based liquefaction potential analyses.
6. The proposed adjustment procedures produce results that can be somewhat conservative for locations where seismicity is dominated by very large historical earthquakes. For such locations, complete performance-based liquefaction potential analyses are recommended.
7. The procedures described in this paper provide a reasonable approximation to a complete, performance-based liquefaction potential evaluation without requiring the user to perform the performance-based calculations. Using a mapped value of required penetration resistance that was obtained by a complete, performance-based analysis, the engineer needs only to compute three adjustment factors using deterministic, algebraic equations.

An effort is currently underway to add N_{req}^{ref} calculation capabilities to the USGS national hazard mapping website. Upon completion, users would be able to enter the latitude and longitude of a site and obtain N_{req}^{ref} values for a return period of interest. The procedures described in this paper could then be used to obtain site-specific required penetration resistances and factors of safety.

The performance-based methodology described in this paper makes use of a recently developed procedure for estimation of the probability of liquefaction. While this procedure is very well suited for implementation into the performance-based methodology, other probabilistic liquefaction procedures could also be used. Similarly, the basic procedure could be extended to use other in situ soil parameters, e.g., CPT tip resistance and shear wave velocity, or to be based upon other ground motion parameters, e.g., Arias intensity (Kayen and Mitchell 1997) or CAV_5 (Kramer and Mitchell 2006).

The intent of this methodology is to make it easier for practicing engineers to realize the benefits of performance-based liquefaction potential procedures, even on routine projects, without having to perform the lengthy performance-based calculations. Performance-based procedures, like all others, still require appropriate characterization of subsurface conditions and careful interpretation of results for proper evaluation of liquefaction hazards.

References

- Atkinson, G. M., Finn, W. D. L., and Charlwood, R. G. (1984). "Simple computation of liquefaction probability for seismic hazard applications." *Earthquake Spectra*, 1(1), 107–123.
- Baker, J. W., and Faber, M. (2008). "Liquefaction risk assessment using geostatistics to account for soil spatial variability." *J. Geotech. Geoenviron. Eng.*, 134(1), 14–23.
- Cetin, K. O., et al. (2004). "Standard penetration test-based probabilistic and deterministic assessment of seismic soil liquefaction potential." *J. Geotech. Geoenviron. Eng.*, 130(12), 1314–1340.
- Cetin, K. O., Der Kiureghian, A., and Seed, R. B. (2002). "Probabilistic models for the initiation of seismic soil liquefaction." *Struct. Safety*, 24(1), 67–82.
- Cornell, C. A. (1968). "Engineering seismic risk analysis." *Bull. Seismol. Soc. Am.*, 58(5), 1583–1606.
- Hwang, J. H., Chen, C. H., and Juang, C. H. (2005). "Liquefaction hazard analysis: A fully probabilistic method." *Proc., Sessions of the Geo-Frontiers 2005 Congress*, R. W. Boulanger et al., eds., ASCE, Reston, Va.
- Idriss, I. M., and Boulanger, R. W. (2004). "Semi empirical procedures for evaluating liquefaction potential during earthquakes." *Proc., 11th Int. Conf. on Soil Dynamics and Earthquake Engineering and 3rd Int. Conf. on Earthquake Geotechnical Engineering*, Vol. 1, Stallion Press, Singapore, 32–56.
- Juang, C. H., and Jiang, T. (2000). "Assessing probabilistic methods for liquefaction potential evaluation." *Soil dynamics and liquefaction*, R. Y. S. Pak and J. Yamamura, eds., ASCE, Reston, Va., 148–162.
- Kayen, R. E., and Mitchell, J. K. (1997). "Assessment of liquefaction potential during earthquakes by Arias intensity." *J. Geotech. Geoenviron. Eng.*, 123(12), 1162–1174.
- Kramer, S. L., and Mayfield, R. T. (2005). "Performance-based liquefaction hazard evaluation." *Proc., Sessions of the Geo-Frontiers 2005 Congress*, R. W. Boulanger et al., eds., ASCE, Reston, Va.
- Kramer, S. L., and Mayfield, R. T. (2007). "Return period of soil liquefaction." *J. Geotech. Geoenviron. Eng.*, 133(7), 802–813.
- Kramer, S. L., and Mitchell, R. A. (2006). "Ground motion intensity measures for liquefaction hazard evaluation." *Earthquake Spectra*, 22(2), 413–438.
- Liao, S. S. C., Veneziano, D., and Whitman, R. V. (1988). "Regression models for evaluating liquefaction probability." *J. Geotech. Eng.*, 114(4), 389–411.
- Marrone, J., Ostadan, F., Youngs, R., and Litehiser, J. (2003). "Probabilistic liquefaction hazard evaluation: Method and application." *Proc., Transactions of the 17th Int. Conf. on Structural Mechanics in Reactor Technology (SMiRT 17)*, International Association of Structural Mechanics in Reactor Technology, Berlin, Germany.
- Martin, G. R., and Lew, M., eds. (1999). *Recommended procedures for implementation of DMG special publication 117—Guidelines for analyzing and mitigating liquefaction hazards in California*, Southern California Earthquake Center, Los Angeles.
- Seed, H. B., and Idriss, I. M. (1971). "Simplified procedure for evaluating soil liquefaction potential." *J. Soil Mech. and Found. Div.*, 107(SM9), 1249–1274.
- Seed, H. B., and Idriss, I. M. (1983). *Ground motions and soil liquefaction during earthquakes*, Earthquake Engineering Research Institute, Berkeley, Calif.
- Seed, H. B., Tokimatsu, K., Harder, L. F., and Chung, R. M. (1985). "Influence of SPT procedures in soil liquefaction resistance evaluations." *J. Geotech. Eng.*, 111(12), 1425–1445.
- Stewart, J. P., Liu, A. H., and Choi, Y. (2003). "Amplification factors for spectral acceleration in tectonically active regions." *Bull. Seismol. Soc. Am.*, 93(1), 332–352.
- Toprak, S., Holzer, T. L., Bennett, M. J., and Tinsley, J. C., III (1999). "CPT- and SPT-based probabilistic assessment of liquefaction." *Proc., 7th U.S.-Japan Workshop on Earthquake Resistant Design of Lifeline Facilities and Countermeasures against Liquefaction*, Multidisciplinary Center for Earthquake Engineering Research, Buffalo, N.Y., 69–86.
- Yegian, M. Y., and Whitman, R. V. (1978). "Risk analysis for ground failure by liquefaction." *J. Geotech. Engrg. Div.*, 104(GT7), 921–938.
- Youd, T. L., et al. (2001). "Liquefaction resistance of soils: Summary report from the 1996 NCEER and 1998 NCEER/NSF workshops on evaluation of liquefaction resistance of soils." *J. Geotech. Geoenviron. Eng.*, 127(10), 817–833.
- Youd, T. L., and Noble, S. K. (1997). "Liquefaction criteria based on statistical and probabilistic analyses." *Proc., NCEER Workshop on Evaluation of Liquefaction Resistance of Soils*, National Center for Earthquake Engineering Research, Buffalo, N.Y., 201–205.